Desalination and Water Treatment
www.deswater.com
doi: 10.5004/dwt.2023.29184

282 (2023) 177–188
January

Natural bentonite used as low-cost adsorbent for the adsorption pretreatment of coal gasification wastewater: performance comparison and component analysis

Huiqin Zhang[a], Renwei Li[a], Biming Liu[b,*], Xian Zhang[c], Guangqing Song[c], Hui Xu[c], Shuo Zhang[c], Lu Chen[c], Shunlong Pan[b], Shengqiang Hei[c,*]

[a]*Hubei Key Laboratory of Ecological Restoration of River-lakes and Algal Utilization, Hubei University of Technology, Wuhan 430068, China, emails: hqzhang@hbut.edu.cn (H. Zhang), l841099130@163.com (R. Li)*
[b]*School of Environmental Science and Engineering, Nanjing Tech University, Nanjing 210009, China, emails: bimingliu@tsinghua.edu.cn (B. Liu), shunlongpan@njtech.edu.cn (S. Pan)*
[c]*State Key Joint Laboratory of Environment Simulation and Pollution Control, School of Environment, Tsinghua University, Beijing 100084, China, emails: heisq17@mails.tsinghua.edu.cn (S. Hei), zhangxian_2016@126.com (X. Zhang), sgq4041@163.com (G. Song), dougherty_xh@163.com (H. Xu), zhangshuoenv@foxmail.com (S. Zhang), chen21@mails.tsinghua.edu.cn (L. Chen)*

Received 2 June 2022; Accepted 3 December 2022

ABSTRACT

Natural clays have the characteristics of wide source, low price, large specific surface area and complex porous structure, and also possess a certain adsorption ability for organics in wastewater. In this study, bentonite (BTT), attapulgite, diatomite and volcanic rock were applied as adsorbents for the pretreatment of coal gasification wastewater (CGW) by batch experiments. Results showed that BTT had better removal performance on chemical oxygen demand (COD), ammoniacal nitrogen (NH_3–N), etc. in CGW after comparison, and the removal efficiencies of COD, NH_3–N, total organic carbon and total phenol could reach 28.1%, 33.5%, 33.9% and 39.6%, respectively. The biodegradability of CGW has been improved after BTT adsorption, and the biochemical oxygen demand (BOD_5)/COD ratio increased from 0.31 to 0.37. Meanwhile, the toxicity of wastewater has been significantly reduced, and the reduction efficiency reached 31.8%. Additionally, the results of kinetics and isotherms implied that the adsorption of organic pollutants is mainly by the monolayer adsorption and diffusion-controlled physical adsorption of BTT. Specifically, the effect of pretreatment is mainly reflected in the adsorption of phenolic pollutants, and the removal of major phenols is the main reason for the reduction of CGW toxicity and the improvement of biodegradability. Hence, BTT as a low-cost adsorbent can provide insight into the wide application of CGW pretreatment.

Keywords: Coal gasification wastewater; Bentonite; Adsorption performance; Phenolic compounds

1. Introduction

Recently, China's energy structure is rich in coal, poor in oil and gas, which determines that energy consumption must be dominated by coal. As an important direction of clean coal conversion and utilization, coal-to-gas industry provides an important solution for the transformation of China's energy development mode [1,2]. Coal gasification wastewater (CGW) produced from coal-to-gas has the characteristics of high concentration of chemical oxygen demand (COD) and ammoniacal nitrogen (NH_3–N), high

* Corresponding authors.

toxicity and poor biodegradability, and contains cyanide, thiocyanate, phenols, polycyclic aromatic hydrocarbon, long-chain alkane and other refractory organics [3]. As a typical refractory industrial wastewater, the treatment of CGW has become an important factor limiting the green development of the coal-to-gas industry.

Phenol/ammonia recovery technology was usually utilized to recover ammoniacal nitrogen and phenols with high concentration from CGW, and greatly reduced the COD, NH_3–N and toxicity of wastewater. However, CGW still had high biological toxicity and poor biodegradability (B/C = 0.3–0.35) after the treatment of phenol/ammonia recovery technology, and the pressure for the stable operation of subsequent biochemical treatment process was still relatively huge [4,5]. Therefore, the biochemical treatment of CGW usually adopts multiple combined processes of anaerobic and oxic, including traditional activated sludge method, anaerobic/anoxic/oxic process, anaerobic sequencing batch reactor (SBR)-oxic, external circulation anaerobic process, enhanced biological process and anoxic/oxic process etc. [6]. The anaerobic process plays a role in the biochemical process, which degrades macromolecular refractory organics into easily degradable small molecular organics through hydrolysis and acidification, thereby improving the biodegradability of wastewater [7]. Additionally, the anaerobic process often has problems such as poor bearing impact load, high toxicity and low treatment efficiency in practical applications, resulting in unstable operation and excessively high concentrations of pollutants in oxic process and even the entire biochemical process [8]. Thus, in order to reduce the influent toxicity of anoxic section, improve its biodegradability, ensure the stable and efficient operation of overall biochemical process, there is an urgent need to seek for new efficient and low-cost pretreatment technology.

CGW is usually pretreated by adsorption method or advanced oxidation processes (AOPs), in which AOPs mainly utilize hydroxyl radicals ($OH^{\bullet}$) etc., to degrade macromolecular refractory or highly toxic organics into low-toxic and easily degradable small-molecular organics [9]. It is often employed for advanced treatment after biochemical treatment due to its high cost, and is rarely used for CGW pretreatment. In the adsorption method, the functional or microporous structure on the surface of adsorbent can adsorb macromolecular refractory organics to achieve the purpose of pretreatment. Activated carbon and activated coke are porous adsorbents with large specific surface area and strong adsorption capacity, and usually used in the pretreatment of CGW [10,11]. Although the treatment efficiency is high, there still suffers from high cost, which limits its large-scale application.

Natural clay materials are naturally existing minerals with large specific surface area and complex porous structure, including bentonite (BTT), attapulgite (ATTP), diatomite (DTT), volcanic (VLN), etc., which have a certain adsorption capacity for heavy metals and organic contaminants in water. Compared with traditional great adsorbents such as activated carbon, the adsorption performance of clays is limited. Modification is often needed to improve their adsorption performance and then applied for the pretreatment of refractory industrial wastewater such as petrochemical wastewater, dye wastewater, pharmaceutical wastewater, etc. [12–14], but the modification also greatly increases the application cost. Nevertheless, unmodified clays have the advantages of natural harmlessness, low price, wide source and distribution, and are potential cheap adsorbents with great application prospects. At present, there is no similar application in the field of CGW pretreatment.

In this study, the pretreatment effects of selective unmodified clay adsorbents (BTT, ATTP, DTT and VLN) on CGW were firstly compared. And specific characterizations of BTT were further analyzed. Then, kinetic and isotherm experiments were carried out to investigate the adsorption process and mechanism of BTT on organics. In the addition, effect of BTT dose was implemented to determine available addition dose. Finally, various analytical methods of water quality (UV/vis, excitation–emission matrix (EEM) and gas chromatograph-mass spectrometer (GC-MS)) was applied to analyze the component variation of CGW before and after adsorption.

2. Materials and methods

2.1. Materials and characterization

The wastewater used in this study was provided by Yima Gasification Plant of Henan Province Gas (Group) Co. (China), and came from the actual CGW influent of anoxic process. This company is one of the earliest and largest coal-to-gas plants in China, and the generated CGW is representative. The water quality of CGW is shown in Table S1 in detail, in which CGW has the high concentration of organic pollutants (COD: 3,132–3,532 mg/L) and low biochemical oxygen demand (BOD_5)/COD ratio (0.34–0.38). Na-BTT, ATTP, DTT, VLN and commercial powdered activated carbon (PAC) were purchased from Henan Zhengzhou Huajing Chemical Co., Ltd. All adsorbents were fully washed with water to remove impurities before use, and then dried in an oven at 105°C for 6 h. The obtained solid was further ground and sieved to 200 mesh. Clays were degassed in a vacuum drying oven (DZF-6020A, LiChen, China) at 200°C for 6 h, and the specific surface and pore diameter were analyzed by a thermogravimetric analyzer (3H-2000PS4, NETZSCH, Germany).

2.2. Batch adsorption experiment

All adsorption experiments were performed in the shaker (HZ-9610 K, China) and carried out under the batch mode. Typically, 250 mL CGW was firstly added to the 500 mL conical flask, and then added 6 g/L adsorbent. The mixture was put into the shaker at 180 rpm, and the temperature was controlled at 25°C for 120 min. At a given interval time, a 10 mL water sample was taken out and filtered through a 0.45 μm membrane for analytical testing. All experimental data of adsorption experiments was analyzed in three parallel groups. The description of kinetic experiment and isotherm experiment were provided in S1 and S2, respectively (Supporting information).

2.3. Characterization of clays

The detailed description about the characterizations of clays was provided in S3, Supporting information.

2.4. Analytical methods

The description of toxicity test about CGW is shown in S4, Supporting information. In order to obtain the composition and characteristics of organics in CGW, EEM was measured by a fluorescence spectrophotometer (Model F-7000, Hitachi, Japan), and the specific operation steps was according to previous study. Specific analyses were performed using region fluorescence integration (RFI), calculated and plotted by Matlab 2019b software. GC-MS (7890A-5975C, Agilent, USA) was used for the analysis of organics composition and content in samples. COD of the sample was measured by dichromate method, the total phenol (Tph) was measured by bromination titration method, NH_3–N was measured by Nessler reagent spectrophotometry. And TOC was measured by total organic carbon analyzer (TOC-LCPH, Shimadzu, Japan), pH (SG2, Hach, USA) and conductivity (S40d, Hach, USA) used the glass electrode method.

3. Results and discussions

3.1. Comparison of the adsorption performance of different clays

The removal efficiency of VLN on COD, TOC, Tph and NH_3–N was less than 10%, and ATTP and DTT also had unsatisfactory removal performance (10%–20%) for CGW (Fig. 1). In contrast, BTT showed relatively high adsorption efficiencies for different pollutants, and relevant COD, TOC, Tph and NH_3–N removal efficiency reached 28.1%, 33.5%, 33.9% and 39.6%, respectively. It can be clearly seen that the CGW chromaticity after BTT adsorption obviously changed from seal brown to pale yellow, and other adsorbents did not cause significant changes in CGW chromaticity (Fig. S1). Besides, VLN exhibited the worst COD, TOC, Tph and NH_3–N removal efficiencies, probably due to its agglomeration in the water body, which resulted in the ineffective contact of VLN with pollutants.

Compared with other adsorbents, BTT has the smallest pore diameter (8.22 nm) and the largest specific surface area (365 m^2/g) and porosity (51.4%) (Table S2). Phenols account for 60%–80% of the total organic pollutants, so the phenols removal is the key to the treatment of CGW. Natural BTT has a large specific surface area and negative charge on the surface, so that it has a great adsorption effect on hydrophilic organics such as phenols [13]. Meanwhile, the negatively charged BTT usually absorbs surrounding cations to maintain electrical balance, such as Ca^{2+} and Na^+, etc [12]. Then, these cations with larger ionic radius can adsorb NH_4^+ through ion exchange, thus ensuring the effective adsorption of NH_3–N while removing organic pollutants. According to the analysis of zeta potential, the pH_{pzc} of all clays was below 7 (Fig. S2). The maximum

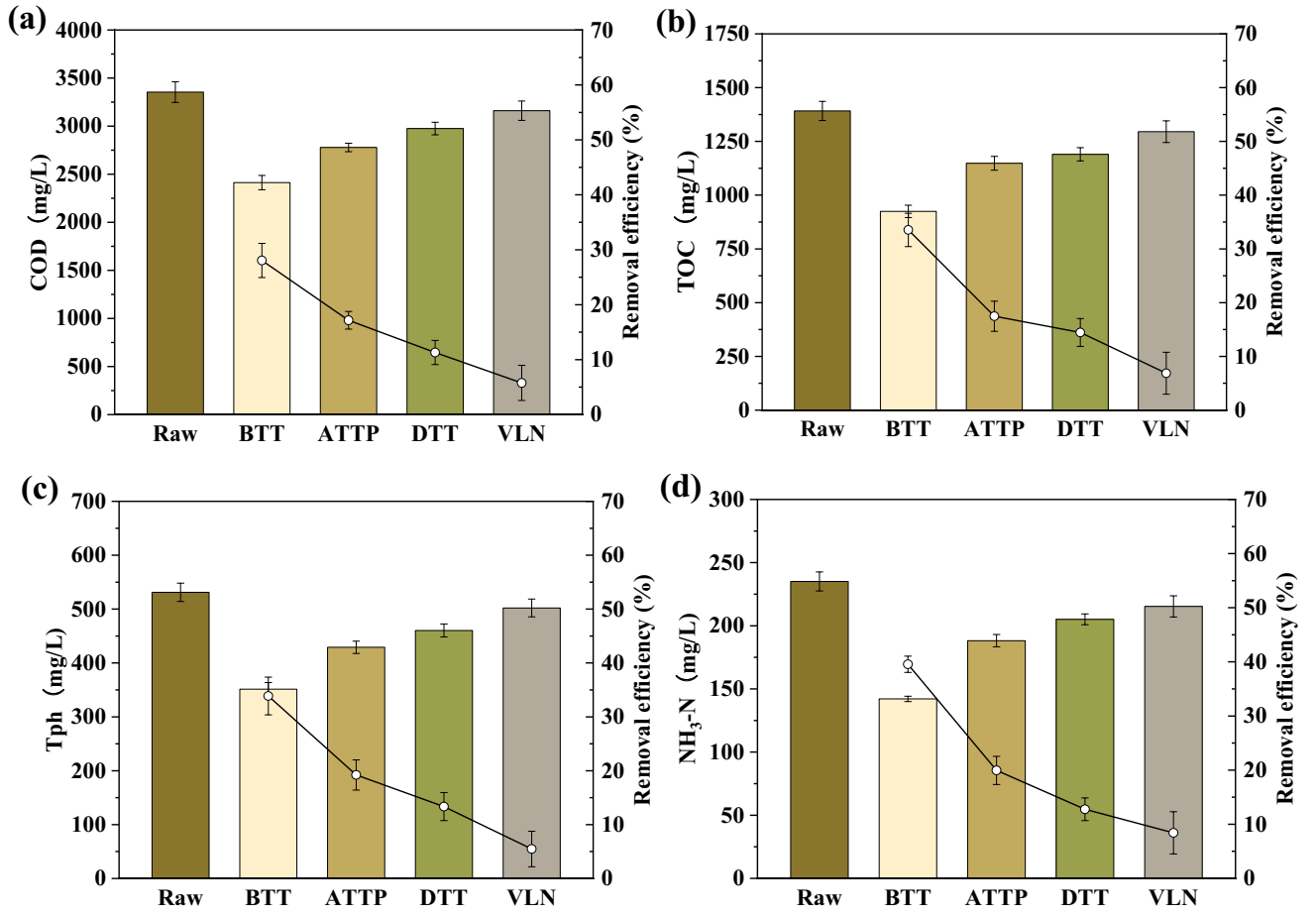

Fig. 1. Comparison of adsorption performance (a) COD, (b) TOC, (c) Tph and (d) NH_3–N on CGW by different clays.

negative zeta potential was obtained for BTT (–14.8 mV) when the pH of solution was 7. And the zeta potentials for ATTP, DTT and VLN were –6.9, –3.7 and –8.5 mV, respectively. As a result, BTT had a higher capacity to adsorb NH_3–N compared to other clays.

The purpose of CGW pretreatment is to reduce the toxicity of wastewater and improve the biodegradability, so as to ensure the stable operation of biochemical process. Whether the biodegradability is improved and the toxicity is reduced is an important basis for evaluating the effectiveness of pretreatment technology. Thus, BOD_5/COD ratio and acute toxicity analysis of luminescent bacteria were used to judge the pretreatment effect of CGW. As shown in Fig. 2, the BOD_5/COD ratio and toxicity unit (TU) of the raw CGW are 0.31 and 22.3, respectively, which belongs to high-acute-toxicity and refractory biodegradable wastewater [15]. Because CGW contained abundant refractory or toxic organic pollutants such as phenols, heterocycles, polycyclic aromatic hydrocarbons and long-chain alkanes, and the main source of biological acute toxicity was phenols [15].

Fig. 2a reveals that BTT, ATTP and DTT all improved the biodegradability of CGW after adsorption, while VLN did not significantly improve the biodegradability. BOD_5/COD ratio of CGW increased from 0.31 to 0.37 by BTT, while ATTP and DTT only increased to 0.34 and 0.32, respectively. Besides, the toxicity of BTT, ATTP and DTT all decreased after adsorption except VLN. BTT still exhibited the strongest detoxification ability, and TU value dropped from 22.3 to 15.2. Although the treated wastewater was still highly toxic, the toxicity of wastewater has been greatly reduced. By contrast, TU value of ATTP and DTT was only reduced to 18.81 and 18.12, respectively. Besides, we utilized PAC as the adsorbent for CGW pretreatment. Results showed that the biodegradability of wastewater was greatly improved and the acute toxicity was significantly reduced, in which BOD_5/COD ratio increased to 0.39 (Fig. S3a), and TU value decreased to 8.81 (Fig. S3b). However, from the perspective of economic analysis, the unit price of BTT (1.7 ¥/kg) is much lower than that of PAC (13 ¥/kg). Thus, the cost of removing COD per kg of BTT is far lower than PAC. Given the above, BTT has a good removal effect on organic pollutants and NH_3–N, and can improve the biodegradability of CGW to the greatest extent and reduce the toxicity. We will discuss the adsorption properties of BTT in detail in the following sections.

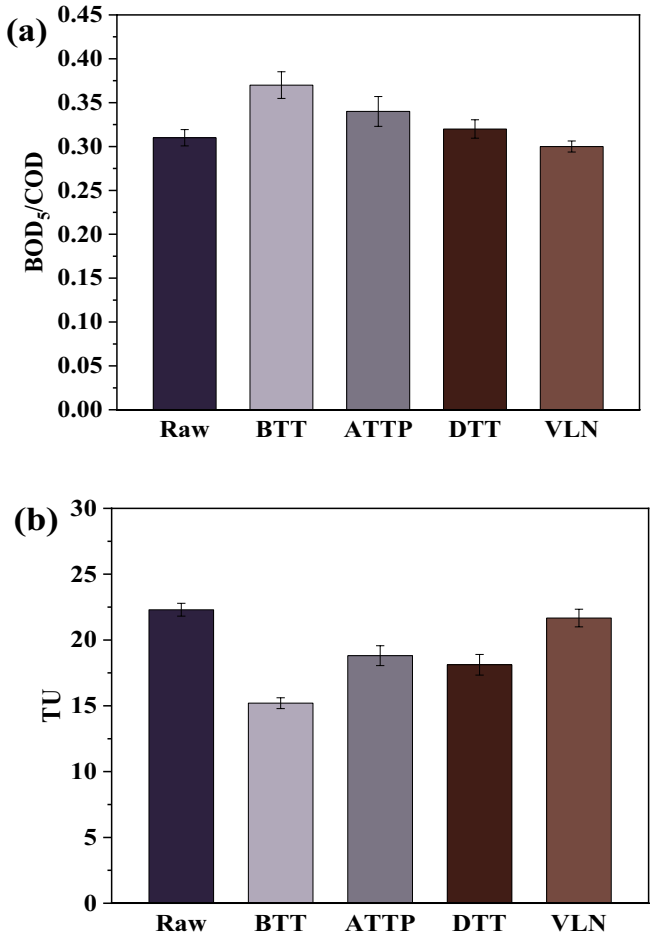

Fig. 2. Comparison of (a) BOD_5/COD ratio and (b) toxicity unit of CGW after different clays adsorption.

3.2. Phase and morphological characteristics of BTT

The metal oxides in BTT mainly contain SiO_2 (59.12%), MgO (16.66%), Fe_2O_3 (3.71%), CaO (1.12%), Al_2O_3 (3.24%), K_2O (0.08%) and Na_2O (6.59%), and the major metal oxides are SiO_2, MgO and Na_2O (Table S3). The high content of Na_2O fraction represents that BTT can effectively adsorb NH_3–N by ion exchange. As the surface morphology of BTT has a direct impact on its ability to adsorb pollutants in water, a scanning electron microscope (SEM) analysis was used to visually determine the aggregation pattern and lamellar structure of BTT. SEM images reflect that BTT is distributed in the form of numerous well-defined fragmentary agglomerates, and there is no connection between them (Fig. S4a). After amplification, the morphology of BTT is similar to cabbage, which is composed of small scales with rough cincinal lamellar structure (Fig. S4b). The overall layer structure appears to be loose, which can make the BTT quickly absorb moisture in the water. Moreover, there is a certain gap between the layers, so it has a relatively large pore and specific surface area, which provides a favorable channel and void structure for its adsorption of pollutants in CGW.

As shown in Fig. S5, 3,439 and 1645 cm^{-1} are the stretching vibration peak and bending vibration peak of O–H, respectively. And 2,923 and 2,856 cm^{-1} are the asymmetric and symmetric stretching vibration peaks of $–CH_2–$. 788 and 1,039 cm^{-1} correspond to Al–O and Si–O groups, respectively, forming the basic Si–O tetrahedral and Al–O octahedral skeleton of BTT. Thus, the stretching vibrations peaks of Si–O–Mg and Si–O–Fe appear at 517 and 464 cm^{-1}. Notably, the stronger Si–O bonds are formed in the structure of BTT. Because the partial entry of Na^+ into the Si–O layer results in a reduction in the charge between the layers and a weakening of the electrostatic interaction, thereby enhancing Si–O bonding energy. Meanwhile, the strong Si–O bonding energy allows for enhanced adsorption on the BTT surface.

3.3. Adsorption kinetics

Adsorption kinetics is mainly utilized to study the diffusion, adsorption performance and mechanism of adsorbate in adsorbent particles [16], and the pseudo-first-order and pseudo-second-order kinetic models were selected to simulate the adsorption process of CGW by BTT. COD adsorption efficiency increased with reaction time, and reached the adsorption equilibrium at 120 min (Fig. 3a). Finally, ~30% of COD adsorption efficiency could be achieved. The fast adsorption rate in the initial stage may be because the organic pollutants are quickly adsorbed by the adsorption sites on the BTT surface. After the surface adsorption sites are occupied, the adsorption rate slows down due to the diffusion resistance until the adsorption is saturated. R^2 of the pseudo-first-order kinetic model (0.9517) is higher than that of pseudo-second-order kinetic model (0.9009), indicating that the pseudo-first-order kinetic model can better describe the adsorption process of CGW by BTT, and q_e calculated by this model is more consistent with the experimental results (Table S4). Hence, the adsorption process is mainly controlled by physical diffusion, which is manifested as a physical adsorption mechanism on the surface and pores of BTT.

3.4. Effect of BTT dose

As BTT dose gradually increased to 10 mg/L, COD value dropped from a rapid decrease to a slow decrease to a stable basically (Fig. 3b). Related COD removal efficiency increased rapidly to 21.7% and then slowly rose to 27.6%. This is because the low dosage of bentonite does not agglomerate, and the adsorption sites on the particle surface and pores can be fully exposed. On the contrary, high dosage of BTT may agglomerate and reduce the specific surface area, resulting in the slowing down of the adsorption rate and the speed of adsorption efficiency. Therefore, in order to save the adsorption cost, we set the BTT dose to 2 g/L in the following experiments.

3.5. Adsorption isotherms

With increased equilibrium concentration of COD, the adsorption capacity of COD by BTT rapidly increased before gradually presenting a gentle trend (Fig. 3c). This finding shows that BTT has a strong affinity and higher adsorption capacity for organics. Adsorption isotherms (e.g., Freundlich and Langmuir) are applied for describing the equilibrium relationship between adsorbent and

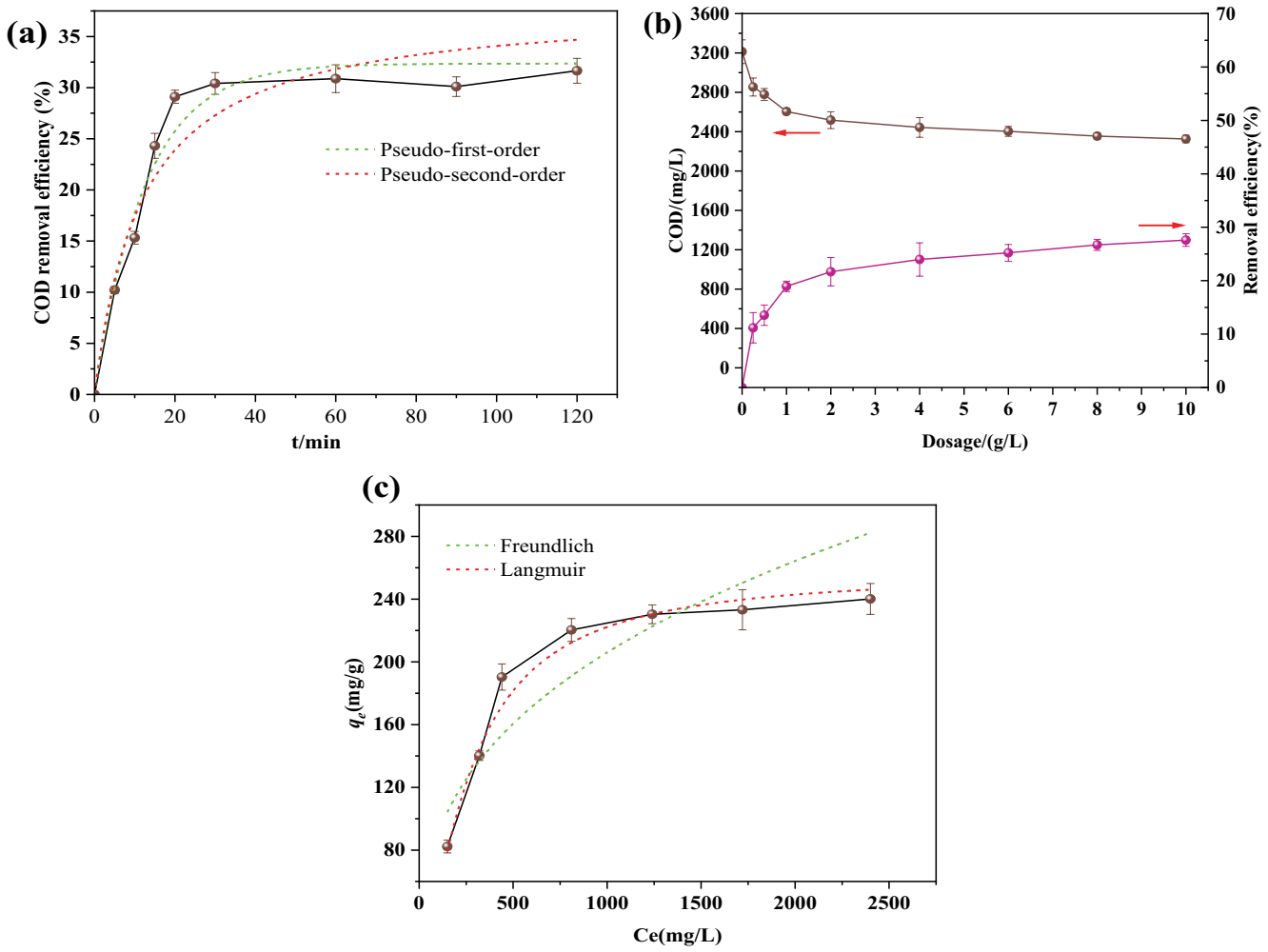

Fig. 3. (a) Adsorption kinetics and (b) effect of absorbent dose and (c) adsorption isotherms of COD removal by BTT.

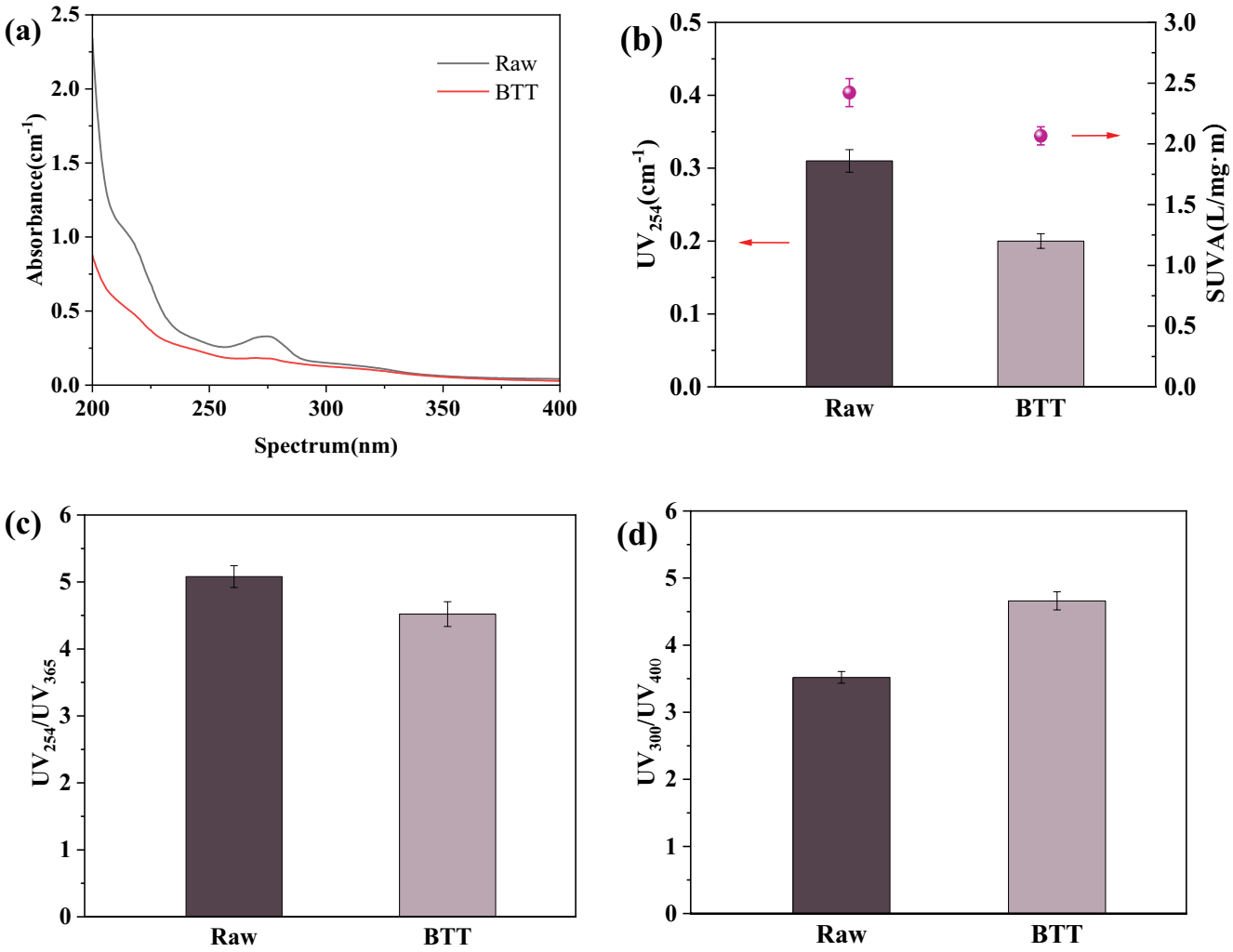

Fig. 4. (a) UV-Vis absorption spectra, (b) UV_{254} and SUVA, (c) UV_{254}/UV_{365} and (d) UV_{300}/UV_{400} CGW by BTT adsorption.

adsorbate, the affinity, and the adsorption capacity of adsorbent. The Langmuir model is based on the assumption that only monolayer adsorption can occur on the adsorbent surface, whereas the Freundlich model provides an empirical description of the equilibrium adsorption of multiple components [17]. R^2 fitted by the Langmuir model is 0.9799, while that by the Freundlich model is only 0.8513 (Table S5). Results implied that Langmuir model could better describe the adsorption process, and uniform monolayer adsorption took place on the adsorption sites of BTT.

3.6. Component variation of CGW by BTT adsorption

Major element content of BTT before and after adsorption is shown in Table S6. Compared with raw BTT, the atomic ratios of C and Na after adsorption change significantly from 56.67 at.% and 16.06 at.% to 69.36 at.% and 4.58 at.%, respectively. It reveals that organics in the CGW is effectively adsorbed, and NH_3–N is immobilized on the BTT surface by ion exchange. Surprisingly, BTT morphology does not change obviously, indicating that the adsorption process does not destroy the BTT structure (Fig. 4c and d).

The organic functional groups will show characteristic absorption bands in the UV-Vis spectrum of CGW, which can express the characteristics of organic pollutants, such as aromaticity. UV-Vis absorption spectra at 200–400 nm before and after adsorption are illustrated in Fig. 4a. CGW has obvious absorption peaks at 200, 220 and 270 nm, indicating that the wastewater mainly contained aromatic compounds. Three absorption peaks correspond to the E1 band (λ_{max} = 184 nm), E2 band (λ_{max} = 204 nm) and B band (λ_{max} = 255 nm) of benzene [18], respectively, demonstrating that aromatic organic compounds have a larger conjugated system than benzene, that is, other electron donating groups are connected to the benzene ring. The absorbance in the range of 200–400 nm was greatly reduced after adsorption, which reflects the great adsorption performance of BTT on aromatic compounds.

Beyond that, other important UV absorption parameters can also reflect the characteristics of dissolved organic matter (DOM) in CGW before and after adsorption from various aspects. UV_{254} is usually used to reflect organic compounds with unsaturated C=C structure in CGW, including aromatic compounds [19]. SUVA is the ratio of UV_{254}

and TOC, which can be used to represent the aromaticity of CGW [20]. Therefore, the levels of UV_{254} and SUVA can jointly reflect the content of aromatic compounds, and the low content of aromatic compounds represents better biodegradability of wastewater. UV_{254} and SUVA were reduced by 35.1% and 14%, respectively, indicating that BTT has a better adsorption effect on aromatic compounds (Fig. 4b). UV_{254}/UV_{365} can describe the proportion of the molecular size of DOM in wastewater, and larger ratio value reveals the higher proportion of small-molecular organic pollutants [21]. Additionally, UV_{300}/UV_{400} is applied to characterize the humification degree of wastewater. Hence, the smaller value of UV_{300}/UV_{400} implies the higher degree of humification, and the more benzene-ring organics exist in wastewater [22]. As the results that UV_{254}/UV_{365} decreased slightly while UV_{300}/UV_{400} increased significantly after adsorption (Fig. 4c and d). In this case, the adsorption performance of BTT on small-molecular organics is better than macromolecular organics, and the concentration of benzene-ring organics is obviously reduced. The major DOM is phenolic compounds (small-molecular organics), it can be inferred that BTT has a great adsorption effect on phenolic substances from the above results.

EEM can represent the change of DOM fluorescence characteristics with excitation and emission wavelengths, and can qualitatively analyze organics in wastewater according to the fluorescence characteristics of different types of organics. As shown in Table S7, RFI divides EEM into five regions, which are aromatic protein I (Region I), aromatic protein II (Region II), fulvic acid (Region III), microbial metabolites (Region IV) and humic acid (Region V) [23].

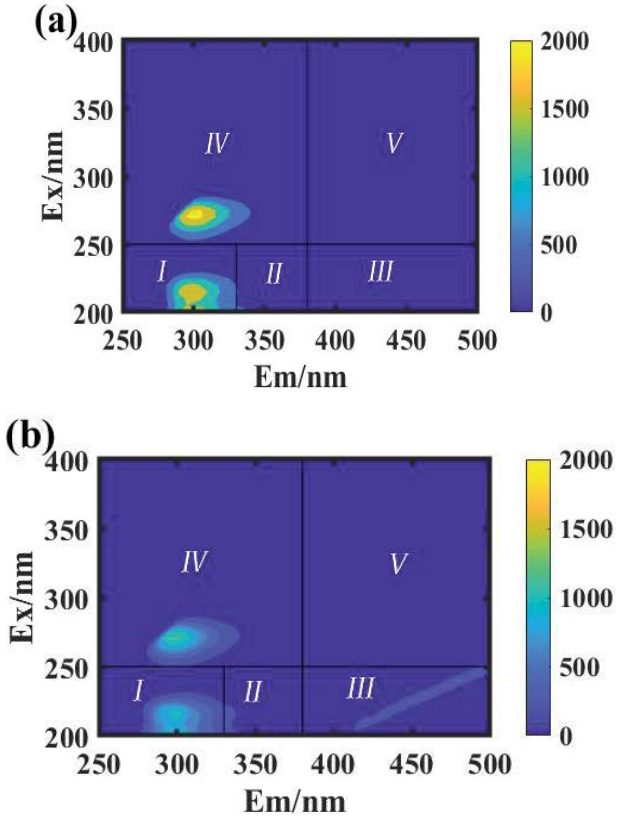

Fig. 5. EEM analysis of CGW (a) before and (b) after BTT adsorption.

Fluorescence peaks of CGW are mainly in the Region I and Region IV, indicating that the organics in CGW are mainly aromatic proteins and microbial metabolites (Fig. 5a). Aromatic proteins generally refer to amino acids with aromatic properties, such as tryptophan and tyrosine. Microbial metabolites can also represent tryptophan-like, tyrosine-like or its residues [24]. The distribution of main fluorescence peaks of CGW EEM is consistent with phenolic substances such as phenol and catechol [25,26], indicating that the main organic pollutants are phenolic compound. Integration and proportion of five fluorescence regions did not change significantly, but the fluorescence intensities of Region I and Region IV decreased significantly by 43% and 45%, respectively (Fig. 5b). Meanwhile, aromatic proteins in Region II also had a removal efficiency of 43%, but the removal of fulvic acid in Region III and humic acid in Region V was unapparent (Table S8). Results also showed that BTT had better adsorption performance on aromatic substances especially phenolic substances.

The components of DOM in CGW were analyzed by GC-MS, and the organics were also were qualitatively detected according to the spectral library (Table S9). Various phenolic substances such as phenol, catechol and alkyl phenols exist in CGW, of which the total proportion of phenolic substances is as high as 65.51%, and the highest proportion of phenol is 28.74%. Surprisingly, the total proportion of phenolic substances decreased to 53.57% after BTT adsorption, and the proportion of various phenols decreased. But heterocyclic organics (e.g., isoquinoline) and long-chain alkanes (e.g., nonadecane) have unsatisfactory removal efficiency, and the proportion of total DOM did not decrease after adsorption. This also reflects that the adsorption ability of BTT for phenolic substances is stronger than other organic contaminants, which also directly leads to the improvement of biodegradability and the reduction of toxicity.

4. Conclusions

CGW chromaticity after BTT adsorption obviously changed from seal brown to pale yellow, and other adsorbents did not cause significant changes in CGW chromaticity. The pseudo-first-order kinetic model can better describe the adsorption process of CGW by BTT, and the adsorption process is mainly controlled by physical diffusion. Results implied that Langmuir model could better describe the adsorption process, and uniform monolayer adsorption took place on the adsorption sites of BTT. The adsorption ability of BTT for phenolic substances is stronger than other organic contaminants, which also directly leads to the improvement of biodegradability and the reduction of toxicity.

Acknowledgments

The authors would like to express gratitude to the National Natural Science Foundation of China (Grant No. 52000102) and the Natural Science Foundation of Jiangsu Province (Grant No. BK20190689) for offering financial support to this research.

References

[1] L. Pan, P. Liu, L. Ma, Z. Li, A supply chain based assessment of water issues in the coal industry in China, Energy Policy, 48 (2012) 93–102.

[2] P. Cui, Y. Qian, S. Yang, New water treatment index system toward zero liquid discharge for sustainable coal chemical processes, ACS Sustainable Chem. Eng., 6 (2017) 1370–1378.

[3] Q. Zhao, Y. Liu, State of the art of biological processes for coal gasification wastewater treatment, Biotechnol. Adv., 34 (2016) 1064–1072.

[4] Q. Ji, S. Tabassum, S. Hena, C.G. Silva, G. Yu, Z. Zhang, A review on the coal gasification wastewater treatment technologies: past, present and future outlook, J. Cleaner Prod., 126 (2016) 38–55.

[5] H.J. Gai, Y.R. Feng, K.Q. Lin, K. Guo, M. Xiao, H.B. Song, X.L. Chen, H. Zhou, Heat integration of phenols and ammonia recovery process for the treatment of coal gasification wastewater, Chem. Eng. J., 327 (2017) 1093–1101.

[6] G. Busca, S. Berardinelli, C. Resini, L. Arrighi, Technologies for the removal of phenol from fluid streams: a short review of recent developments, J. Hazard. Mater., 160 (2008) 265–288.

[7] S. Jia, H. Han, H. Zhuang, B. Hou, K. Li, Impact of high external circulation ratio on the performance of anaerobic reactor treating coal gasification wastewater under thermophilic condition, Bioresour. Technol., 192 (2015) 507–513.

[8] W. Wang, H. Han, Recovery strategies for tackling the impact of phenolic compounds in a UASB reactor treating coal gasification wastewater, Bioresour. Technol., 103 (2012) 95–100.

[9] M. Tong, Pretreatment of Lurgi pressurized coal gasification wastewater by ozone oxidation, Chem. World, 57 (2016) 436–439.

[10] P. Li, N. Ailijiang, X. Cao, T. Lei, P. Liang, X. Zhang, X. Huang, J. Teng, Pretreatment of coal gasification wastewater by adsorption using activated carbons and activated coke, Colloids Surf., A, 482 (2015) 177–183.

[11] H. An, Z. Liu, X. Cao, J. Teng, W. Miao, J. Liu, R. Li, P. Li, Mesoporous lignite-coke as an effective adsorbent for coal gasification wastewater treatment, Environ. Sci. Water Res. Technol., 3 (2017) 169–174.

[12] A. Alshameri, H.P. He, J.X. Zhu, Y.F. Xi, R.L. Zhu, L.Y. Ma, Q. Tao, Adsorption of ammonium by different natural clay minerals: characterization, kinetics and adsorption isotherms, Appl. Clay Sci., 159 (2018) 83–93.

[13] F.A. Banat, B. Al-Bashir, S. Al-Asheh, O. Hayajneh, Adsorption of phenol by bentonite, Environ. Pollut., 107 (2000) 391–398.

[14] E. Bojemueller, A. Nennemann, G. Lagaly, Enhanced pesticide adsorption by thermally modified bentonites, Appl. Clay Sci., 18 (2001) 277–284.

[15] W. Ma, Y. Han, C. Xu, H. Han, H. Zhu, K. Li, M. Zheng, Biotoxicity assessment and toxicity mechanism on coal gasification wastewater (CGW): a comparative analysis of effluent from different treatment processes, Sci. Total Environ., 637–638 (2018) 1–8.

[16] T. He, J.Q. Hua, R.P. Chen, L. Yu, Adsorption characteristics of methylene blue by a dye-degrading and extracellular polymeric substance-producing strain, J. Environ. Manage., 288 (2021) 112446, doi: 10.1016/j.jenvman.2021.112446.

[17] M. Kah, G. Sigmund, F. Xiao, T. Hofmann, Sorption of ionizable and ionic organic compounds to biochar, activated carbon and other carbonaceous materials, Water Res., 124 (2017) 673–692.

[18] W. Ma, Y. Han, C. Xu, H. Han, W. Ma, H. Zhu, K. Li, D. Wang, Enhanced degradation of phenolic compounds in coal gasification wastewater by a novel integration of micro-electrolysis with biological reactor (MEBR) under the micro-oxygen condition, Bioresour. Technol., 251 (2018) 303–310.

[19] P. Xu, H. Han, B. Hou, S. Jia, Q. Zhao, Treatment of coal gasification wastewater by a two-phase anaerobic digestion, Desal. Water Treat., 54 (2014) 598–608.

[20] Q. Ji, S. Tabassum, G. Yu, C. Chu, Z. Zhang, A high efficiency biological system for treatment of coal gasification waste water – a key in-depth technological research, RSC Adv., 5 (2015) 40402–40413.

[21] J.R. Helms, A. Stubbins, J.D. Ritchie, E.C. Minor, D.J. Kieber, K. Mopper, Absorption spectral slopes and slope ratios as indicators of molecular weight, source, and photobleaching of chromophoric dissolved organic matter, Limnol. Oceanogr., 53 (2008) 955–969.

[22] W. Zhang, C. Wei, B. Yan, M. Ren, P. Peng, Composition characterization of dissolved organic matters in coking wastewater, Environ. Chem., 31 (2012) 702–707.

[23] K. Xiao, S. Liang, A.H. Xiao, T. Lei, J.H. Tan, X.M. Wang, X. Huang, Fluorescence quotient of excitation-emission matrices as a potential indicator of organic matter behavior in membrane bioreactors, Environ. Sci. Water Res. Technol., 4 (2018) 281–290.

[24] W. Chen, P. Westerhoff, J.A. Leenheer, K. Booksh, Fluorescence excitation–emission matrix regional integration to quantify spectra for dissolved organic matter, Environ. Sci. Technol., 37 (2003) 5701–5710.

[25] L. Feng, C. Xin, Direct determination of phenol in environmental water by fluorescence spectrophotometry, Spectrolabo, 19 (2002) 267–269.

[26] W.J. Dong, J.P. Song, C. Dong, M.M.F. Choi, Fluorescence quenching method for the determination of catechol with gold nanoparticles and tyrosinase hybrid system, Chin. Chem. Lett., 21 (2010) 346–348.

Supporting information

Appendix S1

Under the conditions of 25°C and 180 rpm, 6 g/L bentonite (BTT) was added to the coal gasification wastewater (CGW) and the reaction was carried out for 120 min to reach the adsorption equilibrium. During the adsorption process, samples were taken at regular intervals through a 0.45 μm membrane to measure the chemical oxygen demand (COD) value. The pseudo-first-order kinetic model [Eq. (1)] and pseudo-second-order kinetic model [Eq. (2)] are the most commonly used kinetic models.

$$\ln\left(q_e - q_t\right) = \ln q_e - k_1 t \tag{S1}$$

where q_e and q_t are the equilibrium adsorption capacity and adsorption capacity (mg/g) at a certain time t (min), respectively, and k_1 is the rate constant of the pseudo-first-order kinetic model (min^{-1}).

$$q_t = \frac{q_e^2 k_2 t}{1 + k_2 q_e t} \tag{S2}$$

where, q_e and q_t are the equilibrium adsorption capacity and adsorption capacity (mg/g) at a certain time t (min), respectively, and k_2 is the rate constant of the pseudo-second-order kinetic model (g/mg·min).

Appendix S2

BTT dose in the CGW was varied in the range of 0–10 g/L, the sample was taken through a 0.45 μm membrane after adsorption equilibrium to determine the equilibrium concentration of COD. Several mathematical models can be

Table S1
Water quality analysis of CGW in this study

Parameter	Value	Parameter	Value
COD (mg/L)	3,132–3,532	Total nitrogen (mg/L)	220.2–265.6
BOD_5 (mg/L)	1,038–1,172	Total phosphorus (mg/L)	1.35–2.57
BOD_5/COD	0.34–0.38	Total phenol (mg/L)	502–564
TOC (mg/L)	1,025–1,239	pH	7.58–7.72
NH_3–N (mg/L)	191.3–237.1	Conductivity (μS/cm)	1,720–1,930

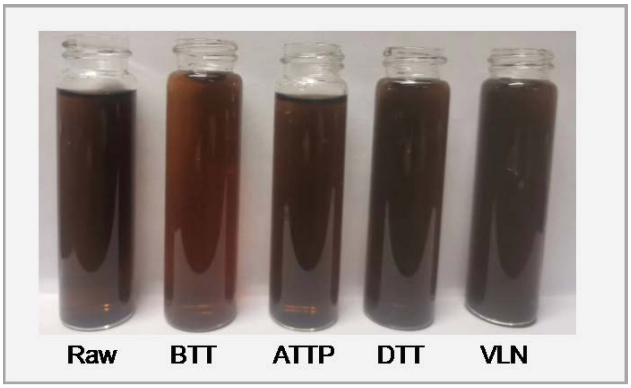

Fig. S1. Color change of CGW after the adsorption of different clays.

Table S2
Specific surface area of clays

Clays	Specific surface area (m^2/g)	Total pore volume (cm^3/g)	Porosity (%)	Pore diameter (nm)
BTT	365	0.15	51.4	8.22
ATTP	30	0.062	42.6	19.21
DTT	46	0.041	31.2	12.31
VLN	17	0.011	40.1	43.11

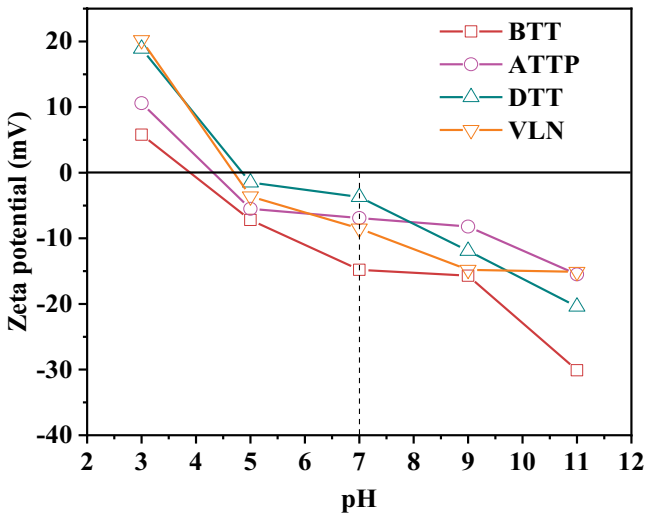

Fig. S2. Zeta potentials of all clays at various pH values.

Table S3
Main chemical oxide components of BTT

Composition	SiO_2	MgO	Fe_2O_3	CaO	Al_2O_3	K_2O	Na_2O
Percentage (wt.%)	59.12	16.66	3.71	1.12	3.24	0.08	6.59

used to quantitatively describe the adsorption isotherm, including Langmuir [Eq. (3)] and Freundlich [Eq. (4)].

$$\text{Langmuir: } q_e = \frac{q_{\max} K_L C_e}{1 + K_L C_e} \tag{S3}$$

$$\text{Freundlich: } q_e = K_F C_e^{1/n} \tag{S4}$$

where q_e and $q_{\max}$ (mg/g) are the equilibrium and the maximum adsorption capacities, respectively (mg/g), C_e represent the concentration of adsorbate in the solution after equilibrium (mg/L), K_L is the Langmuir constant (L/mg), and K_F ((mg/g)/(mg/L)$^{1/n}$) and n are the Freundlich constants representing the affinity between adsorbents and adsorbates and the apparent heterogeneity, respectively. K_L, K_S, K_F, and $1/n$ were obtained after the model fitting.

Appendix S3

The Brunauer–Emmett–Teller test method (ASAP 2020, Micromeritics, USA) was utilized to determine the pore size, pore volume and specific surface area of adsorbents. Zeta potential meter (DelsaNano C, Beckman Coulter, USA) was utilized to measure the zeta potential of adsorbents. X-ray fluorescence (XRF, Thermo, USA)

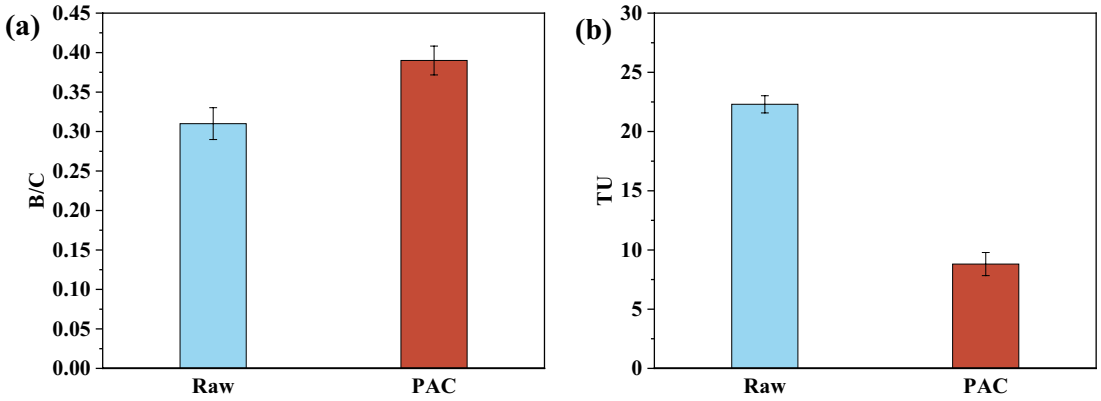

Fig. S3. (a, b) BOD_5/COD ratio and TU value before and after CGW adsorption by commercial PAC.

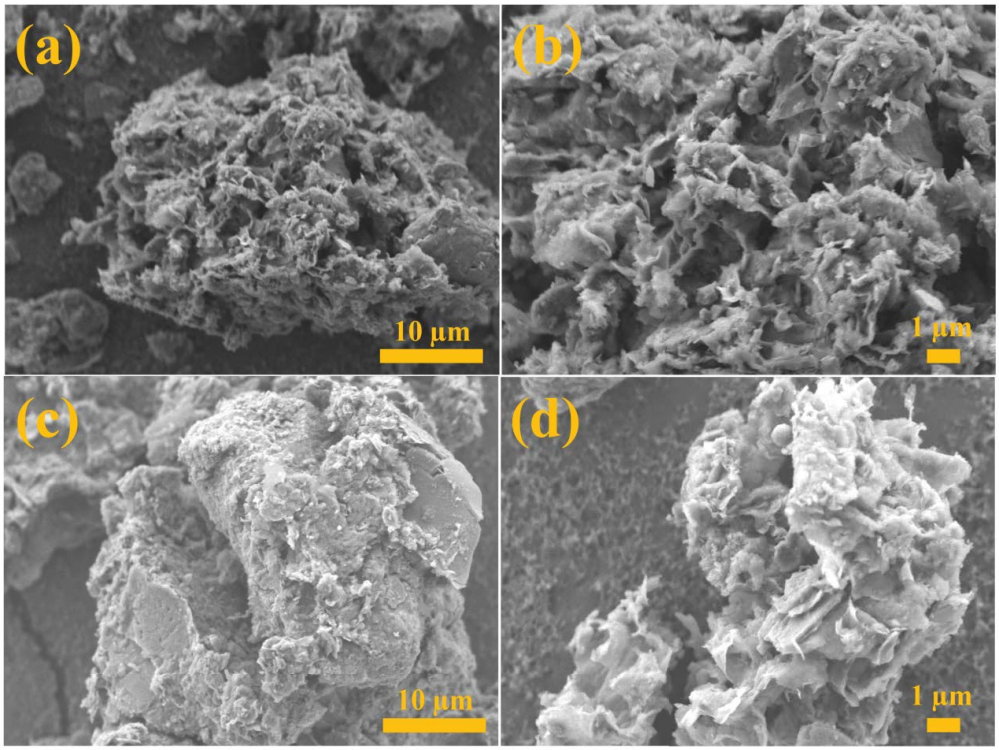

Fig. S4. SEM images of BTT for CGW pretreatment before (a, b) and after (c, d) adsorption.

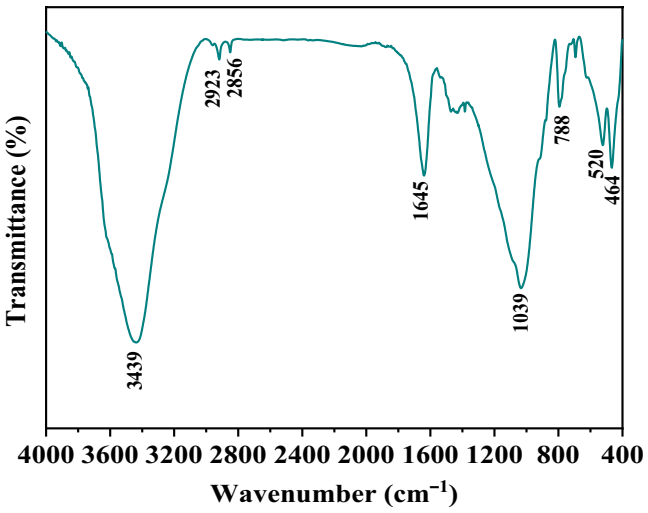

Fig. S5. FT-IR spectrum of BTT.

Table S4
Kinetic parameters for COD adsorption by BTT

Kinetic model	R^2	k_1 (min^{-1})	k_2 (min^{-1})	q_e (mg/g)
Pseudo-first-order	0.9571	0.0795	–	32.35
Pseudo-second-order	0.9009	–	0.0022	38.12

Table S5
Adsorption isotherm parameters of COD adsorption by BTT

Models	Parameters	Value
Langmuir	q_{max} (mg/g)	257.48
	K_L (L/mg)	0.0398
	R^2	0.9799
Freundlich	K_F ((mg/g)/(mg/L)$^{1/n}$)	17.19
	n	2.78
	R^2	0.8513

Table S6
Atomic ratio of BTT before and after adsorption (at.%)

Condition	C	Ca	Fe	Na	Mg
Before	56.67	5.56	6.02	16.06	15.69
After	69.36	5.46	6.62	4.58	13.98

spectrometer was used to detect the content of each metal oxide of BTT. X-ray photoelectron spectroscopy (XPS, ESCALAB 250Xi, Thermo Fisher, USA) was used to detect the chemical element species and their valence states on the surface of BTT. The surface morphology of adsorbent could be directly reflected by a scanning electron microscope (SEM, S-3400N, Hitachi, Japan). By analyzing the changes of characteristic peaks of Fourier-transform infrared spectroscopy (FT-IR, Nicolet iS50, USA), the relevant information of surface functional groups of BTT could be obtained, in order to discuss the chemical effects such as dehydration and dehydrogenation, surface ion exchange, and then explore the adsorption mechanism.

Table S7
Five regions of EMM

Regions	Types of substance	Ex (nm)	Em (nm)
I	Aromatic protein I	200–250	260–320
II	Aromatic protein II	200–250	320–380
III	Fulvic acid	200–250	380–550
IV	Microbial metabolites	250–450	260–380
V	Humic acid	250–450	380–550

Table S8
Integration and proportion of fluorescence region

Index	Sample	I	II	III	IV	V
Regional integration (×106)	Raw	1.75	0.44	0.25	2.10	0.48
	BTT	0.99	0.25	0.51	1.15	0.42
Integration percentage (%)	Raw	55.4	22.3	5.2	13.6	3.4
	BTT	48.2	19.4	16.5	11.4	4.5

Appendix S4

After the lyophilized powder of Vibrio Qinghai was recovered with the resuscitation liquid, the bacterial liquid is inoculated into the sterilized fresh medium for slant subculture. Then the third-generation slant strain was inoculated into a flask and cultured at 150 rpm, 25°C shaker for 30 h to the logarithmic growth phase for the determination of luminescent bacteria toxicity. Different proportions (10%, 20%, 40%, 60%, 80%, and 100%) of water samples were added to the white 96-well plate in turn, and the luminescence intensity (RLU) was tested by a multifunction microplate reader. The luminescent bacteria inhibition rate (η) and toxicity unit (TU) value were calculated as follows:

$$\eta = \left(1 - \frac{RLU_t}{RLU_0}\right) \times 100\% \quad \text{(S5)}$$

$$TU = \frac{1}{EC_{50}} \quad \text{(S6)}$$

where, EC_{50} is the RLU at 50% inhibition.

Table S9
Qualitative analysis of organic composition of CGW before and after BTT adsorption

Organics compounds	Raw CGW (Peak area percentage/%)	BTT adsorption (Peak area percentage/%)
Phenol	28.74	23.22
Catechol	6.78	4.12
Resorcinol	3.21	2.91
Hydroquinone	1.33	1.01
2-Methylphenol	3.82	2.22
4-Methylphenol	14.58	12.32
2,4-Dimethylphenol	1.32	1.21
3,5-Dimethylphenol	2.87	3.32
2,3,5-Trimethylphenol	1.01	1.32
4-Methyl naphthol	0.92	1.11
3,4-Dimethylphenol	0.93	1.22
Oxine	1.23	0.86
Benzopyrrole	3.22	2.85
Isoquinoline	2.11	1.98
Xylene	0.76	2.01
Diphenyl	0.21	0.53
Anthracene	0.15	0.42
Benzofuran	0.18	0.61
Nonadecane	0.78	0.67
Lignocaine	0.56	0.72
Hexatriacontane	0.44	0.71
Others	24.85	34.96